CONTRIBUTI DI RICERCA CRENOS

SPATIAL EFFECTS IN DYNAMIC CONDITIONAL CORRELATIONS

Edoardo Otranto
Massimo Mucciardi
Pietro Bertuccelli

WORKING PAPERS

2014/06

CUEC

CENTRO RICERCHE ECONOMICHE NORD SUD
(CRENoS)
UNIVERSITÀ DI CAGLIARI
UNIVERSITÀ DI SASSARI

CRENOS was set up in 1993 with the purpose of organising the joint research effort of economists from the two Sardinian universities (Cagliari and Sassari) investigating dualism at the international and regional level. CRENoS' primary aim is to improve knowledge on the economic gap between areas and to provide useful information for policy intervention. Particular attention is paid to the role of institutions, technological progress and diffusion of innovation in the process of convergence or divergence between economic areas. To carry out its research, CRENoS collaborates with research centres and universities at both national and international level. The centre is also active in the field of scientific dissemination, organizing conferences and workshops along with other activities such as seminars and summer schools.
CRENoS creates and manages several databases of various socio-economic variables on Italy and Sardinia. At the local level, CRENoS promotes and participates to projects impacting on the most relevant issues in the Sardinian economy, such as tourism, environment, transports and macroeconomic forecasts.

www.crenos.it
info@crenos.it

CRENoS – CAGLIARI
VIA SAN GIORGIO 12, I-09100 CAGLIARI, ITALIA
TEL. +39-070-6756406; FAX +39-070- 6756402

CRENoS - SASSARI
VIA TORRE TONDA 34, I-07100 SASSARI, ITALIA
TEL. +39-079-2017301; FAX +39-079-2017312

Title: SPATIAL EFFECTS IN DYNAMIC CONDITIONAL CORRELATIONS

ISBN: 978 88 84 67 883 6

First Edition: July 2014

Via Is Mirrionis, 1
09123 Cagliari
Tel./Fax 070 291201
www.cuec.it

Spatial Effects in Dynamic Conditional Correlations

Edoardo Otranto
Department of Cognitive Sciences, Educational and Cultural Studies (CSES) and CRENoS,
Università di Messina, Via Concezione, 6 - 98121 Messina, Italy
e–mail: *eotranto@unime.it*

Massimo Mucciardi
Department of Economics, Business, Environmental Sciences and Quantitative Methods (SEAM),
University of Messina, Via Tommaso Cannizzaro, 278 - 98122 Messina, Italy
e–mail: *massimo.mucciardi@unime.it*

Pietro Bertuccelli
Institute for Chemical and Physical Processes,
National Research Council (CNR), V. Stagno D'Alcontres, 37, 98158, Messina, Italy
e–mail: *pietro.bertuccelli@gmail.com*

Abstract

The recent literature on time series has developed a lot of models for the analysis of the dynamic conditional correlation, involving the same variable observed in different locations; very often, in this framework, the consideration of the spatial interactions are omitted. We propose to extend a time-varying conditional correlation model (following an ARMA dynamics) to include the spatial effects, with a specification depending on the local spatial interactions. The spatial part is based on a fixed symmetric weight matrix, called Gaussian Kernel Matrix (GKM), but its effect will vary along the time depending on the degree of time correlation in a certain period. We show the theoretical aspects, with the support of simulation experiments, and apply this methodology to two space-time data sets, in a demographic and a financial framework respectively.

Keywords: space-time correlation; time-varying correlation; weight matrix; gaussian kernel

JEL Classification: C13; C33; C58; J13

1 Introduction

The analysis of space-time series has had a large success in the Eighties, in particular thanks to the extension of the ARMA models to the space-time framework proposed by Pfeifer and Deutsch (1980). Belonging to the ARMA family, a crucial role, in particular for the identification and the residual diagnostic, is played by the autocorrelation function, which is extended to the space-time case using the concept of spatial lag (see, for example, Anselin, 1988a, section 3.1.4). This approach does not consider the fact that correlations are often time-varying.

Generally, the spatial dependence is defined as an effect related to the interaction between geographical or territorial areas and takes place at a particular moment of time. One of the first approaches to the space-time modeling were the autoregressive processes. In the first order spatial autoregressive model (SAR), a variable is a function of its spatial lag at time t. Cressie (1993) proposes a generalization of the STARIMA models presented in Martin and Oeppen (1975) and Pfeifer and Deutsch (1980) such that they also include not only a time-lagged component but also spatial dependence. In quite recent times, there have been several contributions in this field. For example, Elhorst (2001; 2003) presented different single equation models that include a wide range of spatial dependence models. Moreover, space-time dependence is specified in spatial autoregressive models in both theoretical frameworks (Baltagi and Li, 2003 , Pace et al . 1998; 2000) or applications for panel data (Case, 1991; Yilmaz et al 2002 ; Baltagi and Li, 2003; Mobley 2003).

The recent literature has developed several multivariate time series models to represent conditional (on the past) correlations, in particular in a financial framework (see, for example, the review of Bauwens et al., 2006). Very often the variables involved in the analysis represent the same phenomenon referred to different locations, so it is a space-time framework, but the spatial relationships are never considered; for example, many financial applications consider the correlations between pairs of returns of financial indices observed in different countries, without including the spatial effects in the model used.

Notice that the spatial relationships are not necessarily relative to the geographical distance between the countries (as, for example, in Bayoumi et al., 2007, to measure the contagion between financial markets), but they can express an "economic distance"; this idea was developed in this framework, for example, by Otranto (2012), where the distance is linked to the volatility patterns of the returns, or in Borovkova and Lopuhaä (2012), where the weight matrices, used to estimate spatial GARCH models, are based on the inverse travel distance, the GDP and the market capitalization.

A natural extension is to include the spatial effects in the time-varying conditional correlation models. In particular we will use the Tse and Tsui (2002) specification, which provides a direct modelization of the conditional correlation matrix (without a rescaling, as in Engle, 2002) and the introduction of the spatial effects is strictly linked to the Moran local index, one of the most diffused spatial correlation coefficients (see Anselin, 1998a). Also, we specify the family of weight matrices that can be used in our approach to guarantee the definite positiveness of the correlation matrix. This is made by using Gaussian Kernel Functions (GKF) depending on the distance between spatial units. The particular form of the model provides the possibility to test the presence of spatial effects and to calculate the contribution of the spatial effects to the full correlation coefficient at each time. The estimation step requires some reparameterization in the case of a large number N of spatial units; we use a simple reparameterization that reduces the number of unknown coefficients from $N(N-1)/2$ to N.

The paper is organized as follows: next section will contain the description of the model, its characteristics and the estimation procedure; section 3 provides the results of several Monte Carlo experiments to study the behavior of the GKF function, to verify if the likelihood based criteria are useful to select the correct weight matrix and to verify the estimation procedure. Section 4 will present two applications, one in a demographic regional framework and the other in the financial field. Some final remarks will conclude the paper.

2 The Space-Time Conditional Correlation Model

Let $\boldsymbol{y}_t$ be a stationary multivariate random variable relative to N spatial units observed in T time periods ($t = 1, \ldots, T$). We hypothesize that $\boldsymbol{y}_t$ follows a model depending on a set of unknown coefficients $\boldsymbol{\eta} = (\boldsymbol{\eta}'_1, \ldots, \boldsymbol{\eta}'_N)'$, call it $\boldsymbol{y}_t = f(\boldsymbol{Y}_{t-1}; \boldsymbol{\eta}) + \boldsymbol{\varepsilon}_t$, where $\boldsymbol{Y}_t$ represents the information set at time t, or $\boldsymbol{Y}_t = \{\boldsymbol{y}_t, \boldsymbol{y}_{t-1}, \boldsymbol{y}_{t-2}, \ldots\}$. Moreover we hypothesize that the disturbance $\boldsymbol{\varepsilon}_t$ follows a Normal distribution with mean $\mathbf{0}$ so that $(\boldsymbol{y}_t|\boldsymbol{Y}_{t-1}) \sim N(f(\boldsymbol{Y}_{t-1}; \boldsymbol{\eta}); \boldsymbol{D}_t\boldsymbol{R}_t\boldsymbol{D}_t)$, where $\boldsymbol{D}_t$ is a diagonal matrix containing the (time-varying) standard deviations $\sigma_{i,t}$ ($i = 1, \ldots, N$) and $\boldsymbol{R}_t$ is the matrix of correlations between the spatial units at time t (call them $\rho_{ij,t}$; $i, j = 1, \ldots, N$). We suppose that each $\sigma_{i,t}$ depends on a set of parameters $\boldsymbol{\theta}_i$, included in the vector $\boldsymbol{\theta} = (\boldsymbol{\theta}_1, \boldsymbol{\theta}_2, \ldots, \boldsymbol{\theta}_N)$, and $\rho_{ij,t} = h(\boldsymbol{Y}_{t-1}; \boldsymbol{W}; \boldsymbol{\phi})$. The matrix $\boldsymbol{W} = \boldsymbol{W}(\boldsymbol{\xi})$ is a spatial weight matrix which can depend on a set of coefficients ($\boldsymbol{\xi}$), which can also be (partially) coincident with $\boldsymbol{\eta}$ and/or $\boldsymbol{\theta}$; $\boldsymbol{\phi}$ is a set of parameters. In spatial statistics generally the weight matrix is fixed subjectively, using some criteria, such as the neighborhood; anyway we consider a more general case, in which the weights are related to a distance measure which not necessarily represents a geographical distance, depending on the kind of application (for example, in economic application it could be an "economic distance").

The main advantage of the previous hypotheses is that, following the lines of Engle (2002), we can split the log-likelihood in two parts, providing a two-step estimation. In fact, the log-likelihood function is given by:

$$\mathcal{L} = -\frac{1}{2}\sum_{t=1}^{T}\left[Nln(2\pi) + ln\,|\boldsymbol{D}_t\boldsymbol{R}_t\boldsymbol{D}_t| + (\boldsymbol{y}_t - f(\boldsymbol{Y}_{t-1}; \boldsymbol{\eta}))'\boldsymbol{D}_t^{-1}\boldsymbol{R}_t^{-1}\boldsymbol{D}_t^{-1}(\boldsymbol{y}_t - f(\boldsymbol{Y}_{t-1}; \boldsymbol{\eta}))\right]$$

Calling $\boldsymbol{u}_t = \boldsymbol{D}_t^{-1}(\boldsymbol{y}_t - f(\boldsymbol{Y}_{t-1}; \boldsymbol{\eta}))$ the standardized multivariate variable, the previous expression can be rewritten:

$$\begin{aligned}
&\mathcal{L} = -\tfrac{1}{2}\textstyle\sum_{t=1}^{T}\left[Nln(2\pi) + 2ln\,|\boldsymbol{D}_t| + ln\,|\boldsymbol{R}_t| + \boldsymbol{u}'_t\boldsymbol{R}_t^{-1}\boldsymbol{u}_t\right] = \\
&-\tfrac{1}{2}\textstyle\sum_{t=1}^{T}\left[Nln(2\pi) + ln\,|\boldsymbol{D}_t|^2 + (\boldsymbol{y}_t - f(\boldsymbol{Y}_{t-1}; \boldsymbol{\eta}))'\boldsymbol{D}_t^{-1}\boldsymbol{D}_t^{-1}(\boldsymbol{y}_t - f(\boldsymbol{Y}_{t-1}; \boldsymbol{\eta})\right] \\
&-\tfrac{1}{2}\textstyle\sum_{t=1}^{T}\left[-\boldsymbol{u}'_t\boldsymbol{u}_t + ln\,|\boldsymbol{R}_t| + \boldsymbol{u}'_t\boldsymbol{R}_t^{-1}\boldsymbol{u}_t\right] = \\
&\mathcal{L}_1(\boldsymbol{Y}_t; \boldsymbol{\eta}, \boldsymbol{\theta}) + \mathcal{L}_2(\boldsymbol{Y}_t; \boldsymbol{\eta}, \boldsymbol{\theta}, \boldsymbol{\phi})
\end{aligned} \tag{2.1}$$

Recalling that $\boldsymbol{D}_t$ is diagonal, the first component of (2.1) can be written as:

$$\mathcal{L}_1(\boldsymbol{Y}_t; \boldsymbol{\eta}, \boldsymbol{\theta}) = -\frac{1}{2}\sum_{t=1}^{T}\sum_{i=1}^{N}\left[ln(2\pi) + ln(\sigma_{i,t}^2) + \frac{(y_{it} - f(\boldsymbol{Y}_{t-1}; \boldsymbol{\eta}_i))}{\sigma_{i,t}^2}\right]$$

which is the sum of the N log-likelihoods of the single spatial units; it is evident that it depends only on the parameters $\boldsymbol{\eta}$ and $\boldsymbol{\theta}$.

On the other hand the second component of (2.1) contains the parameters $\boldsymbol{\phi}$ of the correlation matrix. This decomposition of the full log-likelihood provides the possibility to perform a two-step estimator for the full set of parameters (Engle, 2002). In the first step we estimate $\boldsymbol{\eta}$ and $\boldsymbol{\theta}$ maximizing (separately) the N univariate models in $\mathcal{L}_1(\boldsymbol{Y}_t; \boldsymbol{\eta}, \boldsymbol{\theta})$. In the second step, given the estimates $\hat{\boldsymbol{\eta}}$ and $\hat{\boldsymbol{\theta}}$, we estimate $\boldsymbol{\phi}$ maximizing $\mathcal{L}_2(\boldsymbol{Y}_t; \hat{\boldsymbol{\eta}}, \hat{\boldsymbol{\theta}}, \boldsymbol{\phi})$.

If the first step provides consistent estimators, the second step will be consistent under not restrictive regularity conditions, as shown in Newey and McFadden (1994).[1]

[1] The regularity (sufficient) conditions require that $\mathcal{L}_2$ is a continuous function in a neighborhood of the true parameters.

The previous result does not require particular assumptions on the correlations; the stronger assumption is that each spatial unit follows a proper dynamics over time, which does not depend on the other spatial units in the mean and in the variance, but only in the correlation structure. This kind of assumption has some common feature with the assumptions of the Seemingly Unrelated Regression Models with spatial correlation (Anselin, 1988b), a frequently used framework in spatial statistics.

A simple and parsimonious way to represent the space-time correlations is to extend the dynamic conditional correlation model of Tse and Tsui (2002), developed for the analysis of the correlation of financial time series, to include the spatial effects. The conditional correlation space-time matrix $\boldsymbol{R}_t$ is represented by the following model:

$$\boldsymbol{R}_t = \boldsymbol{R} + \alpha(\boldsymbol{R}_{t-1} - \boldsymbol{R}) + \beta(\boldsymbol{\Psi}_{t-1} - \boldsymbol{R}) + \gamma(\boldsymbol{W} \circ \boldsymbol{\Psi}_{t-1} - \boldsymbol{R}) \tag{2.2}$$

where $\circ$ represents the element-by-element product (Hadamard product) and α, β, γ are unknown coefficients, whereas $\boldsymbol{\Psi}_t$ is a square positive definite matrix. A sufficient condition to guarantee the stationarity of the model is that the unknown coefficients are non-negative and that $(\alpha + \beta + \gamma) < 1$.

In the original specification of Tse and Tsui (2002) the last term of the right part of (2.2) is not present ($\gamma = 0$) and the so-called correlation targeting is assumed; this means that $\boldsymbol{R}$ is the unconditional correlation matrix, because it is the expected value of both $\boldsymbol{R}_t$ and $\boldsymbol{\Psi}_t$ (for each t). Under this hypothesis $\boldsymbol{R}$ can be estimated by the sample correlation of the standardized residuals $\hat{\boldsymbol{u}}_t$, estimated in the first step (Bollerslev, 1990).[2] In our model this is not possible because the expected value of ($\boldsymbol{W} \circ \boldsymbol{\Psi}_t$) is not $\boldsymbol{R}$. More in general, in (2.2) $\boldsymbol{R}$ is a positive definite matrix with $N(N-1)/2$ unknown coefficients. A dimensionality problem arises when N is not small; we suggest to adopt the following reparameterization:

$$\boldsymbol{R} = \boldsymbol{c}\boldsymbol{c}' + \boldsymbol{\Delta} \tag{2.3}$$

where $\boldsymbol{c} = (c_1, c_2, \ldots, c_N)'$ is a vector of coefficients with $-1 \leq c_i \leq 1$ ($c_i \neq 0$ for each i) and $\boldsymbol{\Delta}$ is a diagonal matrix with the elements on the diagonal equal to $(1 - c_i^2)$. Notice that this reparameterization provides a full rank matrix with diagonal elements equal to 1 and the other elements between -1 and 1, so that $\boldsymbol{R}$ is a $N \times N$ correlation matrix depending on N unknown coefficients.

The matrix $\boldsymbol{\Psi}_t = \{\psi_{ij,t}\}$ is a square positive definite matrix with elements which are functions of the standardized residuals $\hat{\boldsymbol{u}}_t$; following Tse and Tsui (2002), $\psi_{ij,t-1}$ is given by:

$$\psi_{ij,t-1} = \frac{\sum_{k=1}^{K} \hat{u}_{i,t-k}\hat{u}_{j,t-k}}{\sqrt{\sum_{k=1}^{K} \hat{u}_{i,t-k}^2 \sum_{k=1}^{K} \hat{u}_{j,t-k}^2}}$$

A necessary condition for $\boldsymbol{\Psi}_t$ to be positive definite is $K \geq N$. In general, $\boldsymbol{R}_t$ is a well-defined correlation matrix (positive definite with diagonal elements equal to 1) if the starting value $\boldsymbol{R}_0$ and each $\boldsymbol{\Psi}_t$ are well-defined correlation matrices and $\boldsymbol{W}$ is a positive-semidefinite matrix.[3]

We propose to build the exogenous symmetric matrix $\boldsymbol{W}$ in model (2.2) making use of the Gaussian kernel.[4] Considering the positivity of the Gaussian kernel (Hofman et al., 2008,

[2]It differs from the maximum likelihood estimator only in finite sample and provides a large reduction of unknown parameters (Engle and Mezrich, 1996).

[3]In fact the Hadamard product of two positive-semidefinite matrices is positive-semidefinite. This is known as the Schur product theorem (see, for example, Zhang, 2005).

[4]We recall that the classical binary matrices (0-1) are not positive definite by construction.

Fasshauer, 2011), we use a Gaussian Kernel Matrix (GKM) with the weighting function given by:

$$w_{ij} = exp\left\{-0.5\left[d_{ij}/h(d_{ij})\right]^2\right\} \tag{2.4}$$

where d_{ij} is a distance between the generic spatial units i and j and $h(d_{ij})$ is a nonnegative bandwidth function which provides a decay in (2.4) with the increase in the distance. If $i = j$ the value of the weight w_{ij} will be equal to 1. Varying the bandwidth results in a different exponential decay profile, which in turn produces weights that vary more or less rapidly over space. For spatial units far away from i the weight w_{ij} will fall to virtually zero. Among other things, the use of the GKM solves a classic problem in the analysis of spatial data known as topological invariance (Dacey, 1968). As a consequence the function proposed has the important property of being sensitive to topological transformations of the territory.

The dependence of the bandwidth on the distance underlines the importance to link the GKM to the spatial pattern; we have experimented several alternatives and three of them seem to provide better results (other criteria are commented in the final section):

1. $h(d_{ij}) = h_{10p} = 0.1[Max(d_{ij})]$;
2. $h(d_{ij}) = h_{20p} = 0.2[Max(d_{ij})]$;
3. $h(d_{ij}) = h_{Mm} = Maxmin(d_{ij})$.

In the third Maxmin function (Mucciardi and Bertuccelli, 2012) h_{Mm} is chosen in such a way that the following relationship is satisfied:

$$h_{Mm} = max(e_1, e_2, \ldots, e_i, \ldots, e_n) \tag{2.5}$$

where e_i represents the minimum distance of the generic spatial unit i with the other units j (with $i \neq j$). As a consequence each spatial unit is connected to all the others.

Notice that in (2.4), if the distance d_{ij} does not depend on additional parameters, there are not unknown coefficients and $\boldsymbol{\phi} = (c_1, \ldots, c_N, \alpha, \beta, \gamma)'$.[5]

Each element of model (2.2) can be easily interpreted; α represents the coefficient of the time persistence effect, whereas β the coefficient of the time innovation; γ is the coefficient of the spatial effect on the correlation at each time t. Let us consider only the last effect, $\gamma \boldsymbol{W} \circ \boldsymbol{\Psi}_{t-1}$; each row of this matrix is given by:

$$\gamma \frac{\sum_{k=1}^{K} w_{ij} \hat{u}_{i,t-k} \hat{u}_{j,t-k}}{\sqrt{\sum_{k=1}^{K} \hat{u}_{i,t-k}^2 \sum_{k=1}^{K} \hat{u}_{j,t-k}^2}}$$

The local Moran index (Anselin, 1995) for unit i is used to represent the spatial correlation coefficient between i and the other units, and it is given by $\sum_{j=1}^{N} w_{ij} \hat{u}_{i,t-k} \hat{u}_{j,t-k}$. As a consequence, each row of $\boldsymbol{W} \circ \boldsymbol{\Psi}_{t-1}$ contains an information linked to the local spatial correlations calculated in the last K periods.

In particular we can interpret the ratio (multiplied by 100) between the element (i, j) of $\gamma \boldsymbol{W} \circ \boldsymbol{\Psi}_{t-1}$ and the element (i, j) of $\boldsymbol{R}_t$ as the percentage of correlation at time t due to the spatial effect. Notice also that the Tse-Tsui model (without correlation targeting) is nested in model (2.2), so that we can verify the hypothesis of no significance of the spatial effect, $\gamma = 0$, by a simple $t-$ratio or a likelihood ratio test.

[5]If d_{ij} depends on $\boldsymbol{\xi} \subset (\boldsymbol{\eta}, \boldsymbol{\theta})$, it is estimated in the first step, otherwise $\boldsymbol{\xi}$ will be included in $\boldsymbol{\phi}$.

3 Monte Carlo Evidence

We have performed some simulation experiments with the following purposes:

1. verify the behavior of the GKM functions in correspondence of the three different bandwidths;

2. verify the importance by considering the correct model specification and the possibility of detecting it in statistical terms;

3. verify the goodness of the reparameterization (2.3) in the estimation step.

First, we have randomly generated a different number N of spatial units ($N = 5$, 10, 25, 50, 100) and the relative distance matrix in a lattice of dimension 200×200, using an ad hoc Matlab function. For each spatial pattern we have calculated the three bandwidths h_{10p}, h_{20p} and h_{Mm} and synthesized these results in Table 1, where the averages and the standard deviations of the 1000 coefficients are shown. Notice as the average value of the bandwidth coefficient increases for h_{10p} and h_{20p} when N increases and vice versa for h_{Mm}, with a similar average value with respect to h_{10p} when $N = 100$; also the bandwidth is more stable when N increases, as shown by a low standard deviation.

In Figure 1 we show the behavior of the three different GKM functions with bandwidths equal to the average values reported in Table 1. It is clear how the GKM with bandwidth h_{Mm} changes its behavior with a curve which approaches the GKM with h_{10p} when the number of spatial units increases (in the case of 100 spatial units the two lines are almost overlapping).

Second, we have generated space-time series with $T = 500$ and $N = 10$ and 25 from model (2.2), fixing $\alpha = 0.5$, $\beta = 0.1$, $\gamma = 0.3$, using the previous spatial patterns. Subsequently the GKM with the three different bandwidths was applied to the distance matrices.

The matrix $\boldsymbol{R}$ has also been generated randomly and it changes in each simulation to verify the robustness of the estimation of the dynamic coefficients. It was generated through a Matlab function following the work of Numpacharoen and Atsawarungruangkit (2012). Finally we have generated the standardized residuals $\hat{\boldsymbol{u}}_t$ from a multivariate standard Normal distribution and obtained the $\boldsymbol{R}_t$ matrices.

The simulation experiment consists of generating 200 space-time series using each one of the three previous specifications of the weight matrix; moreover we also generate data from a model without spatial effects ($\gamma = 0$), labeled with "Time". Then we have estimated model (2.2) with the four specifications and compared them in terms of the Bayesian Information Criterion (BIC) and percentage of Mean Absolute Error (MAE). For the sake of simplicity, at this stage the matrix $\boldsymbol{R}$ is considered known. In Table 2 we show the results. It can be seen that the BIC favors clearly the true model; in some cases the h_{20p} and the h_{Mm} are confused; this is due to the similar bandwidth coefficient and, as a consequence, the similar behavior of the two kernels (cf. Table 1 and Figure 1). The MAE demonstrates the cases of similar fitting performance of the alternative models; notice that the presence of spatial effects implies that the space–time models clearly outperform the model "Time" with differences of more than 10 percentage points. Also, when the true model is "Time", it is important to notice that the difference among the four models is not relevant in terms of MAE; in fact, in this case, the parameter γ is approximately equal to zero in the space-time models. On the other hand the fact that it is not present in the model is well evidenced from the BIC, which clearly favors the model "Time". Again the MAE indicates a similar performance of models with weight matrix h_{20p} and h_{Mm}. The spatial dimension does not seem to affect the results, which are very similar for $N = 10$ and $N = 25$. To summarize, this experiment shows that the BIC is able to detect the presence of spatial effects in model (2.2) and the correct weight matrix; the MAE results show that the consideration of spatial effects is relevant in capturing the correct behavior of the correlations.

In the third experiment, we want to verify the goodness of the reparameterization (2.3) in the estimation step. We have generated 200 space-time series with $T = 500$ and $N = 10$ and 25 from model (2.2) similarly to the previous experiment, with weight matrix obtained from the GKM function with bandwidth h_{20p}. Then we have estimated model (2.2) using three alternatives for the matrix $\boldsymbol{R}$:

1. "True $\boldsymbol{R}$": we consider $\boldsymbol{R}$ known, using the true one used to generate the data, as in the previous simulation experiment;

2. "Sample $\boldsymbol{R}$": we consider the sample correlation of the $\hat{\boldsymbol{u}}_t$, as under the correlation targeting hypothesis;

3. "Repar. $\boldsymbol{R}$": we estimate $\boldsymbol{R}$ using the reparameterization (2.3).

In Table 3 we show the results of this third set of simulations for the dynamic parameters; the bias of the "Sample $\boldsymbol{R}$" estimation is evident because, as said previously, in model (2.2) $\boldsymbol{R}$ can not be considered as the unconditional correlation. The similar estimation obtained from "True $\boldsymbol{R}$" and "Repar. $\boldsymbol{R}$", which on average show estimates near the true data generating parameters is relevant. The estimates of "Repar. $\boldsymbol{R}$" do not worsen when the spatial dimension increases (and increasing the number of estimated coefficients from 13 to 28), indeed they seem more robust than the "True $\boldsymbol{R}$" estimates. This result seems to support the use of parameterization (2.3) as a good parsimonious approximation of the matrix $\boldsymbol{R}$.

4 Applications

We apply the proposed conditional correlation model to two space-time series, in which the spatial component has a different interpretation. In the first case (analysis of Italian births) it has a "classical" interpretation, namely it is territorial distance between pairs of regions; in the second case (analysis of financial markets) it can be interpreted as an "economic distance" because the relationship depends on the similarity of the volatility of each pair of markets. The first example is mainly used to illustrate the procedure of model selection and the output of the model proposed, whereas the second one is used to derive some information for a more accurate portfolio selection.

4.1 Correlation between regional Italian births

We have considered the space-time series of Italian crude birth rate[6] from January 2003 to November 2013 (monthly data) for the 20 Italian Regions (Istat source[7]). In Italy the 20 Regions are frequently grouped in 4 wide areas with similar cultural, economic, social, demographic characteristics (they are depicted in Figure 2):

- Northern Italy: it consists of 8 regions: Valle d'Aosta (VAL), Piedmont (PIE), Liguria (LIG), Lombardy (LOM), Emilia-Romagna (EMI), Veneto (VEN), Friuli-Venezia Giulia

[6] Crude birth rate indicates the number of live births occurring during the year, per 1,000 population estimated at midyear.

[7] The data are available at the website http://demo.istat.it.

(FRI), Trentino Alto-Adige (TRE). Further aggregation includes the first four regions in the Northwest Italy and the last four regions in the Northeast Italy. This distinction is less clear for Emilia-Romagna, whose territory stretches from west to east Italy.

- Central Italy: it encompasses four regions: Lazio (LAZ), Marche (MAR), Tuscany (TUS), Umbria (UMB). Historically, also Romagna (the part of Emilia-Romagna bordering Marche and Tuscany) is part of Central Italy.
- Southern Italy: it encompasses 6 regions: Abruzzo (ABR), Apulia (APU), Basilicata (BAS), Calabria (CAL), Campania (CAM), Molise (MOL). From a geographical perspective, Abruzzo is part of the Central Italy, but the traditions, history, culture, dialect are typical of South Italy.
- Insular Italy: it includes the two major islands of Italy, Sicily (SIC) and Sardinia (SAR). Particularly, the latter has traditions and culture different from the rest of the Italian regions. Southern and Insular Italy (with the southern part of Lazio) constitute the so–called Mezzogiorno, approximately overlapping (except Sardinia) with the historical Kingdom of Two Sicilies.

We have applied model (2.2), using the three different kernel functions to obtain $\boldsymbol{W}$ and the "Time" specification with $\gamma = 0$.[8] In the first–step estimation we have simply considered constant means and variances.

In Table 4 we show the estimation results of the four models; the constant part (coefficients c_i, $i = 1, \ldots, 20$) does not show relevant differences among the models. All the models do not find a significant α coefficient, so that the autoregressive component of the conditional correlation is not present, whereas it depends on the correlations in the most recent periods. The spatial effects are significant in the three space-time models (coefficients γ significant); as expected the coefficient β of the Time specification is greater than the corresponding coefficient of the space–time models because it also contains the not–explicit spatial effects. In terms of fitting we can notice that the space–time models have a lower BIC with respect to the Time specification and the model with the $\boldsymbol{W}$ matrix derived from the bandwidth h_{Mm} is the best one. Based on the simulation results of Section 3, it can be adopted as the model to represent the conditional correlations.

Following this model, it results that the conditional correlation is, on average, frequently more than 0.7 for several pairs of regions (see Table 5); the only regions which seem to have a small linear relationship with the others are Valle d'Aosta (the smallest region with strong components of native culture) and Lazio (the region containing Rome, the Italian city with more interracial relationships). The regions with the highest conditional correlation in the time span considered are Lombardy and Veneto (on average it is 0.93), whereas the ones with the lowest conditional correlation are Valle d'Aosta and Lazio (on average 0.30). In Figure 4 we can notice the different dynamics of the two conditional correlation series: we notice an approximately constant behavior of the first series and more oscillations of the second one, which seems to follow the economic business cycle fluctuations.

In Table 6 the average percentage of the spatial effects for each correlation coefficient (ratio between each element of $\gamma \boldsymbol{W} \circ \boldsymbol{\Psi}_{t-1}$ and the corresponding element of $\boldsymbol{R}_t$) is shown. In several cases, on average, the percentage of spatial effects on the full conditional correlation is more

[8]The GKM functions are applied to the 20 Italian regions with a maximum extension of 1065 kilometers. The distance matrix is calculated on the territorial barycenters of the regions. The three bandwidths coefficients are (in kilometers) $h_{10p} = 106.47$, $h_{20p} = 212.93$ and $h_{Mm} = 378.74$ respectively.

than 7% and characterizes several regions belonging to the same wide area; the highest average percentage is shown by the pair Abruzzo–Molise with 7.77%, whereas the minimum by the pair Sicily–Valle d'Aosta, which are two opposite regions in cultural, economic and social terms. For the two previous pairs, we can notice the presence of a strong spatial effect for the pair Lombardy–Veneto (7%, on average, of the full correlation) and a weak spatial effect in the case of Valle d'Aosta–Lazio (1.12% on average). Anyway the linear correlation coefficient between the elements of Table 5 and 6 is very small (0.13). In other words, for this application it seems that the time and spatial effects are clearly separated: high level of the full conditional correlation do not correspond to high levels of the contribution of the spatial effect to the full conditional correlation. This can be made clearer deriving the dendrograms from Tables 5 and 6, using the corresponding entries as measures of similarity between each pair of regions (Figure 4). We can cut the dendrograms to obtain three groups; in the first case, obtained from the averages of conditional correlations (left panel), the group containing only VAL and LAZ is the one with lower levels of conditional correlations; then there is another small group (composed by MOL, ABR, BAS, TRE, UMB) with the regions showing an average correlation between 0.6 and 0.7 and a third large group with the regions with larger correlation with the other regions. The right panel, based on the dendrogram derived from the average percentages of spatial effects in the correlation, shows how the groups are strictly linked to geographical distances.

4.2 Correlation between financial indices

As previously said, distance is not necessarily a geographical concept but it could represent the degree of similarity of economic behaviors. A recent matter in the econometric literature is given by the estimation of the conditional correlations of a set of assets or indices in the financial analysis. This is an important issue because the correct estimation of the covariance matrix of this set of variables helps in portfolio risk evaluation and asset allocation. We consider the series of returns of the set of financial indices available in the *Oxford-Man Institute's Realised Library* version 0.2, which collects data relative to the main financial indices in the world. In particular we have considered the common dates from July 8, 2002 to May 23, 2014 (1962 daily observations) of the following 21 indices: S&P 500 (USA); FTSE 100 (England); Nikkei 225 (Japan); DAX (Germany); Russell 2000 (USA); All Ordinaries (Australia); DJIA (USA); Nasdaq 100 (USA); CAC 40 (France); Hang Seng (China); Kospi Composite (South Korea); AEX (Holland); Swiss Market Index (Switzerland); IBEX 35 (Spain); S&P CNX Nifty (India); IPC (Mexico); Bovespa (Brasil); S&P/TSX Composite (Canada); Euro STOXX 50 (Europe); FT Straits Times (Singapore); FTSE MIB (Italy).

A recent strand of the literature has the purpose of detecting the determinants of financial market correlations. Many authors indicate volatility as the main cause of the correlation and some authors have tried to include its effect in conditional correlation models (see, for example, Bauwens and Otranto, 2013); the idea is that similar volatility patterns can have similar correlation dynamics. A common assumption is to consider constant means and time–varying conditional variances.

We specify the space–time conditional correlation model considering the dependence of the matrix $\boldsymbol{W}$ on a measure of distance between volatilities relative to a pair of markets. For this purpose we use the GARCH distance proposed by Otranto (2008) following these steps:

1. estimate the conditional variance of each series of returns using a GJR–GARCH(1,1)

model (see Glosten et al., 1993); the model is given by:

$$r_{i,t} = \mu_i + \varepsilon_{i,t}$$

$$\sigma^2_{i,t} = \omega_i + a_i \varepsilon^2_{i,t-1} + b_i \sigma^2_{i,t-1} + g_i \delta_{i,t-1} \varepsilon^2_{i,t-1}$$

$$\delta_{i,t} = \begin{cases} 1 & \text{if } r_{i,t} < 0 \\ 0 & \text{if } r_{i,t} \geq 0 \end{cases}$$

where $r_{i,t}$ represents the return of the series i at time t, $\varepsilon_{i,t} \sim N(0, \sigma^2_{i,t})$ and $\sigma^2_{i,t}$ represents the conditional variance of the return at time t; μ_i, ω_i, a_i, b_i, g_i are unknown coefficients. The square root of $\sigma^2_{i,t}$ is the i-th element of the diagonal of $\boldsymbol{D}_t^{1/2}$. The presence of the dummy variable $\delta_{i,t}$ indicates the presence of asymmetric effects due to negative returns, which provide higher levels of volatility;

2. estimate the GARCH (euclidian) distance for each pair of series (i, j):

$$\left[(a_i + g_i/2)^2/(1 - b_i^2) + (a_j + g_j/2)^2/(1 - b_j^2) - 2(a_i + g_i/2)(a_j + g_j/2)/(1 - b_i b_j)\right]^{1/2}$$

3. Calculate $\boldsymbol{W}$ using the previous distances and estimate the series $\boldsymbol{R}_t$.

In terms of the notation of section 2 we have $\boldsymbol{\eta} = (\mu_1, \ldots, \mu_N)'$, $\boldsymbol{\theta}_i = (\omega_i, a_i, b_i, g_i)'$, $\boldsymbol{\xi} = (a_1, b_1, g_1, \ldots, a_N, b_N, g_N)$ ($\boldsymbol{\xi} \subset \boldsymbol{\theta}$).

To save space we do not show the estimation results (available on request) to obtain the four alternative conditional correlation series (obtained with the three different bandwidths of the kernel function and the specification without spatial effects); the results indicate that the γ coefficient is significant in the three space-time specifications and that the model with the h_{10p} bandwidth is the one with the lowest BIC.[9]

To perform a comparison between the alternative models it may be more interesting to compare them in terms of portfolio performance criteria than statistical criteria. Following Engle and Colacito (2006), we consider a set of identical expected returns for all the competing models and perform the portfolio allocation selecting the vector of weights at time t, call it $\boldsymbol{p}_t$, solving the classical variance minimization problem subject to a required return equal to 1 (Markowitz, 1959):

$$\boldsymbol{p}_t = \frac{\boldsymbol{\Sigma}_t^{-1}\boldsymbol{r}}{\boldsymbol{r}'\boldsymbol{\Sigma}_t^{-1}\boldsymbol{r}}$$

where $\boldsymbol{r}$ is the vector of expected returns. The portfolio weights depend on the expected returns, the variances, and the correlations of the financial indices; since the expected returns and the conditional variances are identical for all the models, the comparisons will depend only on the differences in the correlation matrices. To select the theoretical expected returns we follow again the suggestion of Engle and Colacito (2006), considering hedging portfolios, obtained by setting one entry of $\boldsymbol{r}$ equal to 1 and the others equal to zero; in this way the index with unitary weight is hedged against all other indices. The best model will be the one with the smallest portfolio volatility (square root of portfolio variance) for each vector of expected returns.

In Table 7 we show a synthesis of the results. In order to ease the comparison we set the lowest volatility as equal to 100 in each experiment. Of course the differences are not so relevant

[9]The four values of the BIC are: 2.78 for the case h_{10p}, 2.80 for h_{20p}, 2.82 for h_{Mm}, 2.84 for $Time$.

because the conditional correlation models differ only in the bandwidth or the presence of the spatial coefficient. It is remarkable that, consistent with the BIC results, the space-time model with bandwidth h_{10p} has the minimum portfolio variance in 10 of the 21 theoretical portfolios, whereas the model without the spatial component is consistent in only 2 of the theoretical portfolios. Moreover the average of all the portfolio variances is smaller for the h_{10p} case. In other words it seems that the consideration of the volatility distance between the financial markets improves the asset allocation performance by reducing the portfolio variance.

5 Final Remarks

This paper introduces a new approach of measuring space-time conditional correlation which provides time–varying correlation coefficients with spatial effects. The model proposed is an extension of the Tse and Tsui (2002) model for the analysis of the dynamic conditional correlation in financial markets. It is possible to extend other approaches to the space-time case (for example the so-called DCC model of Engle, 2002); our preference for the Tse-Tsui model is due to the fact that the presence of the matrix of innovations $\boldsymbol{\Psi}_t$, combined with the spatial weight matrix $\boldsymbol{W}$, provides a convenient interpretation because each element of the resulting matrix is linked to the spatial local Moran index. In practice in the same model we can combine time-varying and spatial effects which have a proper interpretation also when we consider them separately.

The estimation of the model does not present particular drawbacks; it is possible to use the MLE with the Quasi MLE interpretation, which ensures consistent estimates. We propose the bandwidth $h(d_{ij})$ (present in the kernel function which generates the matrix $\boldsymbol{W}$) with three alternative functions; the choice favors the possibility of linking the bandwidth to the spatial units by the distance. This approach differs fundamentally from other approaches (called data-driven) that require use of intensive computational methods for the estimation of the bandwidth (see Silverman, 1986, Wand and Jones, 1995). Of course it is also possible to substitute $h(d_{ij})$ with an unknown coefficient h, inserting it in the set of parameters present in the likelihood. We have tried to perform this approach in the two applications illustrated in section 4; it is interesting to note that in both the cases the BIC obtained is higher than the BIC of the best model derived from our procedure and that the inference does not differ substantially between the two approaches, in spite of different estimates of the bandwidth. In particular, the bandwidth obtained with our procedure for the first application was $h_{Mm} = 378.74$ whereas with the MLE it was $h_{MLE} = 616.54$; in the second application we have obtained $h_{10p} = 0.017$ and $h_{MLE} = 0.10$. This result seems to support the idea that the distance-based bandwidth choice is a simple valid solution and that the estimation of the coefficient does not involve significant improvements in fitting.

The applications performed confirm that the consideration of spatial effects in time–varying correlation dynamics can increase the fitting of the data (lower BIC), provide some useful interpretation (percentage of the spatial effects in respect to the full correlation in the demographic application) and can increase the performance of the model in inferential exercises such as in better portfolio allocation in financial applications.

References

[1] Anselin, L. (1988a). *Spatial Econometrics: Methods and Models*. Kluwer, Dordrecht.

[2] Anselin, L. (1988b). A test for spatial auto-correlation in seemingly unrelated regressions. *Economics Letters* 28, 335–341.

[3] Anselin, L. (1995). Local indicators of spatial association LISA. *Geographical Analysis* 27, 93–115.

[4] Baltagi, B.H., Li, D. (2003). Prediction in the panel data model with spatial correlation. In: Anselin, L., R.Florax Rey, S. (Eds.), *New Advances in Spatial Econometrics*, Springer-Verlag, 283–296.

[5] Bauwens, L., Laurent, S., Rombouts, J.V.K. (2006). Multivariate GARCH models: a survey. *Journal of Applied Econometrics*, 21, 79–109.

[6] Bauwens, L., Otranto, E. (2013). Modeling the dependence of conditional correlations on volatility. *CORE Discussion Papers* 2013/14, Université catholique de Louvain, Center for Operations Research and Econometrics (CORE).

[7] Bayoumi, T., Fazio, G., Kumar, M., MacDonald, R. (2007). Fatal attraction: using distance to measure contagion in good times as well as bad, *Review of Financial Economics*, 16, 259–273.

[8] Bollerslev, T. (1990). Modelling the coherence in short-run nominal exchange rates: a multivariate generalized ARCH approach. *Review of Economics and Statistics*, 72, 498-505.

[9] Borovkova, S. and Lopuhaä, R. (2012): Spatial GARCH: a spatial approach to multivariate volatility modeling. Available at SSRN: http://ssrn.com/abstract=2176781.

[10] Case, A. (1991). Spatial patterns in household demand. *Econometrica*, 59, 953–965.

[11] Cressie, n. (1993). *Statistics for Spatial Data*. Wiley, New York, 1993.

[12] Dacey, M. F. (1968). A review on measures of contiguity for two and k-color maps. In Berry, B.J.L., Marble, D.F. (Eds.): *Spatial Analysis: A Reader in Statistical Geography*. Englewood Cliffs, NJ: Prentice-Hall, 479–495,.

[13] Elhorst, J.P., 2001 Dynamic models in space and time. *Geographical Analysis*, 33, 119–140.

[14] Engle, R.F. (2002). Dynamic conditional correlation: a simple class of multivariate generalized autoregressive conditional heteroskedasticity models. *Journal of Businsess and Economic Statistics*, 20, 339–350.

[15] Engle, R., Colacito, R. (2006). Testing and valuing dynamic correlation for asset allocation. *Journal of Business and Economic Statistics*, 24, 238–253.

[16] Engle, R.F., Mezrich, J. (1996). GARCH for groups. *Risk*, 9, 36–40.

[17] Fasshauer, G.E. 2011. Positive definite kernels: past, present and future. *Dolomites Research Notes on Approximation*, 4, 21-63.

[18] Glosten, L., Jagannathan, R. and Runkle, D. (1993). On the relation between expected value and the volatility of the nominal excess return on stocks. *Journal of Finance*, 48, 1779–1801.

[19] Hofmann, T., Scholkopf, B., Smola, A. J. (2008). Kernel methods in machine learning. *Annals of Statistics*, 36, 1171–1220

[20] Markowitz, H, (1959). *Portfolio Selection: Efficient Diversification of Investments*. Wiley, New York.

[21] Martin, R., and J. Oeppen (1975). The identification of regional forecasting models using space–time autocorrelation functions. *Transactions of the Institute of British Geographers*, 70, 330-349.

[22] Mobley, L.R. (2003). Estimating hospital market pricing: an equilibrium approach using spatial econometrics. *Regional Science and Urban Economics*, 33, 489-516.

[23] Mucciardi, M., Bertuccelli, P. (2012). The impact of the weight matrix on the local indicators of spatial association: an application to per-capita value added in Italy. *International Journal of Trade and Global Markets*, 5, 133–141.

[24] Newey, W., McFadden, D. (1994). Large sample estimation and hypothesis testing. In Engle, R.F., McFadden, D. (Eds.): *Handbook of Econometrics* (Vol. 4). New York: Elsevier Science, 2113–2245.

[25] Numpacharoen K., Atsawarungruangkit A. (2012). Generating correlation matrices based on the boundaries of their coefficients. *PLoS ONE*, 7, e48902. doi:10.1371/journal.pone.0048902.

[26] Otranto, E. (2008) Clustering heteroskedastic time series by model-based procedures. *Computational Statistics and Data Analysis*, 52, 4685–4698.

[27] Otranto, E. (2012), A GARCH-variance dependent approach to modelize dynamic conditional correlations. *Journal of Applied Statistical Sciences*, 20, 101–118.

[28] Pace, R. K., Barry, R., Clapp, J. M., Rodriguez M. (1998). Spatio–temporal autoregressive models of neighborhood effects. *Journal of Real Estate Finance and Economics*, 17, 15–33.

[29] Pace, R. K., Barry, R., Gilley, O. W., Sirmans, C. F. (2000). A method for spatial–temporal forecasting with an application to real estate prices. *International Journal of Forecasting*, 16, 229–246.

[30] Pfeifer, P.E, Deutsch, S.J. (1980). Identification and interpretation of first order space time ARMA. *Technometrics* 22, 397–408.

[31] Silverman, B.W. (1986). *Density Estimation*. Chapman Hall, London.

[32] Tse, Y.K., Tsui, A.K.C. (2002). A multivariate generalized autoregressive conditional heteroscedasticity model with time- varying correlations. *Journal of Businsess and Economic Statistics*, 20, 351–362.

[33] Yilmaz, S., Haynes, K.E., Dinc, M. (2002). Geographic and network neighbors: Spillover effects of telecommunications infrastructure. *Journal of Regional Science*, 42, 339–360.

[34] Wand, M.P., Jones, M.C. (1995). *Kernel Smoothing*. Chapman Hall/CRC, London.

[35] Zhang, F. (2005). *The Schur Complement and its Applications*. Springer, New York.

TABLES AND FIGURES

Table 1: Simulation results: average and standard deviation (in parentheses) of three kinds of bandwidths in correspondence of 1000 simulated spatial patterns in a 200×200 lattice with different number N of spatial units .

N	h_{10p}	h_{20p}	h_{Mm}
5	17.38	34.76	95.02
	(3.17)	(6.34)	(29.72)
10	20.21	40.43	75.47
	(2.33)	(4.66)	(19.65)
25	22.92	45.84	52.61
	(1.64)	(3.29)	(11.44)
50	24.45	48.91	39.88
	(1.29)	(2.58)	(8.05)
100	25.55	51.09	29.62
	(0.96)	(1.91)	(4.82)

Table 2: Simulation results: percentage of the Space-Time conditional correlation models showing the best BIC and average of the MAE (multiplied by 100) in correspondence of different bandwidths of the weight matrix and different number of spatial units ($T = 500$; number of replications 200; size of the lattice 200×200).

	10 spatial units							
	Percentage best BIC				MAE average			
True	h_{10p}	h_{20p}	h_{Mm}	Time	h_{10p}	h_{20p}	h_{Mm}	Time
h_{10p}	99.5	0.0	0.5	0.0	1.06	3.68	4.65	11.83
h_{20p}	0.0	84.5	15.5	0.0	3.48	0.90	1.90	11.18
h_{Mm}	0.0	12.5	87.5	0.0	3.76	1.57	0.90	10.24
Time	0.5	1.0	0.5	98.0	0.74	0.65	0.67	0.63
	25 spatial units							
	Percentage best BIC				MAE average			
True	h_{10p}	h_{20p}	h_{Mm}	Time	h_{10p}	h_{20p}	h_{Mm}	Time
h_{10p}	100.0	0.0	0.0	0.0	0.62	2.94	2.49	11.48
h_{20p}	0.0	86.0	14.0	0.0	2.53	0.53	0.94	9.92
h_{Mm}	0.5	13.0	86.5	0.0	2.16	1.00	0.55	10.20
Time	0.0	0.0	0.0	100.0	0.29	0.35	0.27	0.25

The matrix $\boldsymbol{R}$ is generated at each replication. h_{10p}, h_{20p}, h_{Mm} indicate the different specifications of the bandwidth to obtain the weight matrix illustrated in Section 2. “Time” represents the case without spatial effects ($\gamma = 0$ in 2.2).

Table 3: Simulation results: averages (standard deviation in parentheses) of the estimated parameters of the Space-Time conditional correlation models with different estimation method for the constant matrix $\boldsymbol{R}$ and different number of spatial units ($T = 500$; number of replications 200; size of the lattice 200×200).

		10 spatial units			25 spatial units		
Coefficient	True	True $\boldsymbol{R}$	Sample $\boldsymbol{R}$	Repar. $\boldsymbol{R}$	True $\boldsymbol{R}$	Sample $\boldsymbol{R}$	Repar. $\boldsymbol{R}$
α	0.5	0.48 (0.06)	0.46 (0.07)	0.47 (0.06)	0.46 (0.08)	0.42 (0.09)	0.47 (0.09)
β	0.1	0.10 (0.02)	0.14 (0.02)	0.10 (0.02)	0.11(0.02)	0.14 (0.02)	0.11 (0.02)
γ	0.3	0.31 (0.04)	0.25 (0.05)	0.31 (0.04)	0.33 (0.05)	0.25 (0.04)	0.32 (0.05)

The matrix $\boldsymbol{R}$ is generated at each replication. The weight matrix is obtained from the GKM function with bandwidth h_{20p}. “True $\boldsymbol{R}$” means that in the estimation we use the same generated $\boldsymbol{R}$, “Sample $\boldsymbol{R}$” means that $\boldsymbol{R}$ is estimated using the sample correlation, “Repar. $\boldsymbol{R}$” means that $\boldsymbol{R}$ is estimated using the reparameterization (2.3).

Table 4: Regional Italian crude births: Estimation results (standard errors in parentheses) of the space–time–varying conditional correlation using different weight matrix specifications, and corresponding Log-Likelihood and BIC.

Coefficient	h_{10p}		h_{20p}		h_{Mm}		$Time$	
α	0.000	(0.002)	0.000	(0.000)	0.000	(0.002)	0.000	(0.000)
β	0.083	(0.028)	0.051	(0.027)	0.040	(0.028)	0.158	(0.028)
γ	0.081	(0.013)	0.069	(0.010)	0.079	(0.012)		
c_1	0.946	(0.015)	0.934	(0.013)	0.930	(0.013)	0.906	(0.015)
c_2	0.569	(0.070)	0.559	(0.068)	0.560	(0.068)	0.559	(0.070)
c_3	0.992	(0.009)	0.974	(0.007)	0.971	(0.006)	0.955	(0.008)
c_4	0.835	(0.030)	0.821	(0.029)	0.815	(0.030)	0.810	(0.031)
c_5	0.991	(0.008)	0.972	(0.007)	0.967	(0.007)	0.962	(0.007)
c_6	0.929	(0.017)	0.921	(0.015)	0.916	(0.015)	0.896	(0.017)
c_7	0.932	(0.017)	0.916	(0.016)	0.908	(0.016)	0.888	(0.019)
c_8	0.967	(0.010)	0.954	(0.009)	0.949	(0.009)	0.937	(0.011)
c_9	0.937	(0.017)	0.921	(0.015)	0.912	(0.015)	0.905	(0.016)
c_{10}	0.813	(0.034)	0.802	(0.033)	0.792	(0.033)	0.785	(0.035)
c_{11}	0.938	(0.016)	0.922	(0.015)	0.911	(0.015)	0.904	(0.016)
c_{12}	0.594	(0.065)	0.588	(0.062)	0.585	(0.061)	0.557	(0.068)
c_{13}	0.838	(0.031)	0.821	(0.029)	0.815	(0.029)	0.802	(0.031)
c_{14}	0.776	(0.039)	0.762	(0.038)	0.753	(0.038)	0.737	(0.042)
c_{15}	0.975	(0.011)	0.956	(0.010)	0.948	(0.010)	0.929	(0.012)
c_{16}	0.986	(0.010)	0.973	(0.008)	0.969	(0.008)	0.938	(0.011)
c_{17}	0.865	(0.025)	0.857	(0.024)	0.853	(0.025)	0.840	(0.027)
c_{18}	0.967	(0.015)	0.951	(0.011)	0.943	(0.011)	0.916	(0.014)
c_{19}	0.965	(0.016)	0.960	(0.013)	0.960	(0.012)	0.912	(0.015)
c_{20}	0.942	(0.019)	0.937	(0.017)	0.925	(0.017)	0.889	(0.019)
Log-Lik.	368.22		385.73		390.52		341.17	
BIC	-5.17		-5.46		-5.54		-4.77	

Table 5: Regional Italian crude births: Average conditional correlation derived from the space–time model with h_{Mm} bandwidth.

	VAL	LOM	TRE	VEN	FRI	LIG	EMI	TUS	UMB	MAR	LAZ	ABR	MOL	CAM	APU	BAS	CAL	SIC	SAR
PIE	0.50	0.90	0.73	0.88	0.82	0.84	0.87	0.83	0.71	0.81	0.51	0.71	0.65	0.82	0.83	0.73	0.81	0.82	0.81
VAL		0.52	0.44	0.52	0.48	0.49	0.51	0.48	0.42	0.48	0.30	0.42	0.39	0.49	0.49	0.44	0.48	0.49	0.47
LOM			0.78	0.93	0.87	0.87	0.91	0.87	0.74	0.86	0.54	0.75	0.68	0.86	0.87	0.76	0.84	0.86	0.84
TRE				0.78	0.74	0.72	0.76	0.72	0.62	0.72	0.44	0.63	0.58	0.72	0.73	0.65	0.70	0.71	0.69
VEN					0.88	0.85	0.91	0.86	0.75	0.86	0.53	0.76	0.69	0.86	0.88	0.77	0.84	0.85	0.84
FRI						0.80	0.85	0.80	0.70	0.81	0.51	0.72	0.65	0.82	0.83	0.73	0.80	0.81	0.79
LIG							0.85	0.81	0.69	0.80	0.51	0.70	0.64	0.81	0.82	0.71	0.79	0.80	0.80
EMI								0.86	0.74	0.86	0.53	0.76	0.68	0.86	0.86	0.76	0.83	0.84	0.83
TUS									0.72	0.82	0.53	0.72	0.66	0.82	0.83	0.73	0.80	0.81	0.81
UMB										0.71	0.45	0.64	0.59	0.72	0.73	0.64	0.71	0.71	0.70
MAR											0.53	0.74	0.68	0.84	0.85	0.74	0.81	0.82	0.80
LAZ												0.46	0.42	0.53	0.54	0.47	0.52	0.54	0.52
ABR													0.61	0.77	0.78	0.68	0.74	0.74	0.72
MOL														0.71	0.72	0.64	0.69	0.68	0.65
CAM															0.91	0.80	0.88	0.88	0.83
APU																0.82	0.90	0.89	0.84
BAS																	0.79	0.78	0.73
CAL																		0.89	0.82
SIC																			0.84

Table 6: Regional Italian crude births: Average percentage of spatial effects of each conditional correlation derived from the space–time model with h_{Mm} bandwidth.

	VAL	LOM	TRE	VEN	FRI	LIG	EMI	TUS	UMB	MAR	LAZ	ABR	MOL	CAM	APU	BAS	CAL	SIC	SAR
PIE	4.81	7.29	5.34	5.56	4.11	7.63	6.48	5.68	4.18	3.96	2.92	2.48	1.63	1.22	0.65	0.63	0.31	0.27	2.47
VAL		5.37	5.54	4.20	3.01	5.01	4.74	3.58	2.60	2.66	1.12	1.45	1.19	0.67	0.30	0.44	0.15	0.12	0.99
LOM			6.87	7.00	5.93	7.00	7.23	6.05	4.52	5.03	3.56	3.30	2.12	1.66	1.02	0.91	0.43	0.30	1.90
TRE				7.37	7.06	5.18	6.31	4.79	4.17	4.81	2.27	3.11	2.60	1.49	1.09	1.05	0.36	0.19	1.02
VEN					7.23	5.62	7.39	6.08	5.68	6.09	3.47	4.51	3.31	2.41	1.81	1.61	0.75	0.40	1.67
FRI						4.15	6.23	4.81	4.71	5.37	3.32	4.13	3.11	2.17	1.88	1.58	0.71	0.32	1.06
LIG							6.85	6.38	4.84	4.92	4.34	3.31	2.27	1.95	1.11	0.97	0.57	0.52	3.42
EMI								7.34	6.34	6.99	4.54	5.58	3.99	3.21	2.20	2.00	1.12	0.77	2.94
TUS									7.54	6.98	6.85	5.64	4.63	3.79	2.72	2.46	1.57	1.34	3.94
UMB										7.21	6.57	7.02	6.62	4.95	3.98	3.72	2.79	1.90	4.01
MAR											6.89	7.32	6.52	5.34	4.48	4.07	2.60	1.73	3.26
LAZ												5.87	5.25	4.99	4.66	3.25	3.31	3.56	4.66
ABR													7.77	7.29	6.16	5.93	4.50	2.93	3.71
MOL														7.72	6.77	7.07	5.38	3.36	2.76
CAM															7.13	7.17	6.62	4.79	3.10
APU																7.10	6.58	4.01	1.79
BAS																	6.91	4.23	1.84
CAL																		6.09	1.83
SIC																			2.93

Table 7: Financial indices: Comparison of volatilities for each theoretical portfolio.

hedged index	h_{10p}	h_{20p}	h_{Mm}	$Time$
S&P 500	100.00	100.43	100.62	100.79
FTSE 100	100.00	100.18	100.29	100.12
Nikkei 225	100.22	100.15	100.06	100.00
DAX	100.51	100.00	100.02	100.48
Russel 2000	100.00	100.58	100.97	101.69
All Ordinaries	100.07	100.06	100.06	100.00
DJIA	100.00	100.62	101.04	101.38
Nasdaq 100	100.00	100.40	100.73	101.38
CAC 40	100.00	100.63	100.68	100.34
Hang Seng	100.22	100.15	100.00	100.04
KOSPI	100.05	100.02	100.00	100.02
AEX	101.36	100.23	100.00	100.34
Swiss Market	100.04	100.00	100.04	100.48
IBEX 35	100.00	100.26	100.46	100.26
S&P CNX Nifty	100.00	100.05	100.15	100.10
IPC	100.21	100.00	100.03	100.64
Bovespa	100.06	100.00	100.02	100.48
S&P/TSX	100.00	100.37	100.44	100.34
Euro STOXX 50	100.56	100.11	100.00	101.07
FT Straits Times	100.22	100.14	100.00	100.01
FTSE MIB	100.00	100.22	100.35	100.63
Average	100.17	100.22	100.28	100.51

The lowest volatility in each minimum variance portfolio experiment is set to 100 and then the average is computed for each model, so a number like $(100+x)$ means that the corresponding model provides, on average, a $x\%$ higher portfolio volatility than the model having the lowest volatility.

Figure 1: Behavior of GKM functions with different bandwidths in correspondence of different numbers of spatial units. The lines refer to three GKM functions with bandwidth h_{10p} (black line), h_{20p} (gray line), h_{Mm} (dotted line). The values of the bandwidths are reported in Table 1. The y–axis refers to the weight w, the x–axis refers to the distance d.

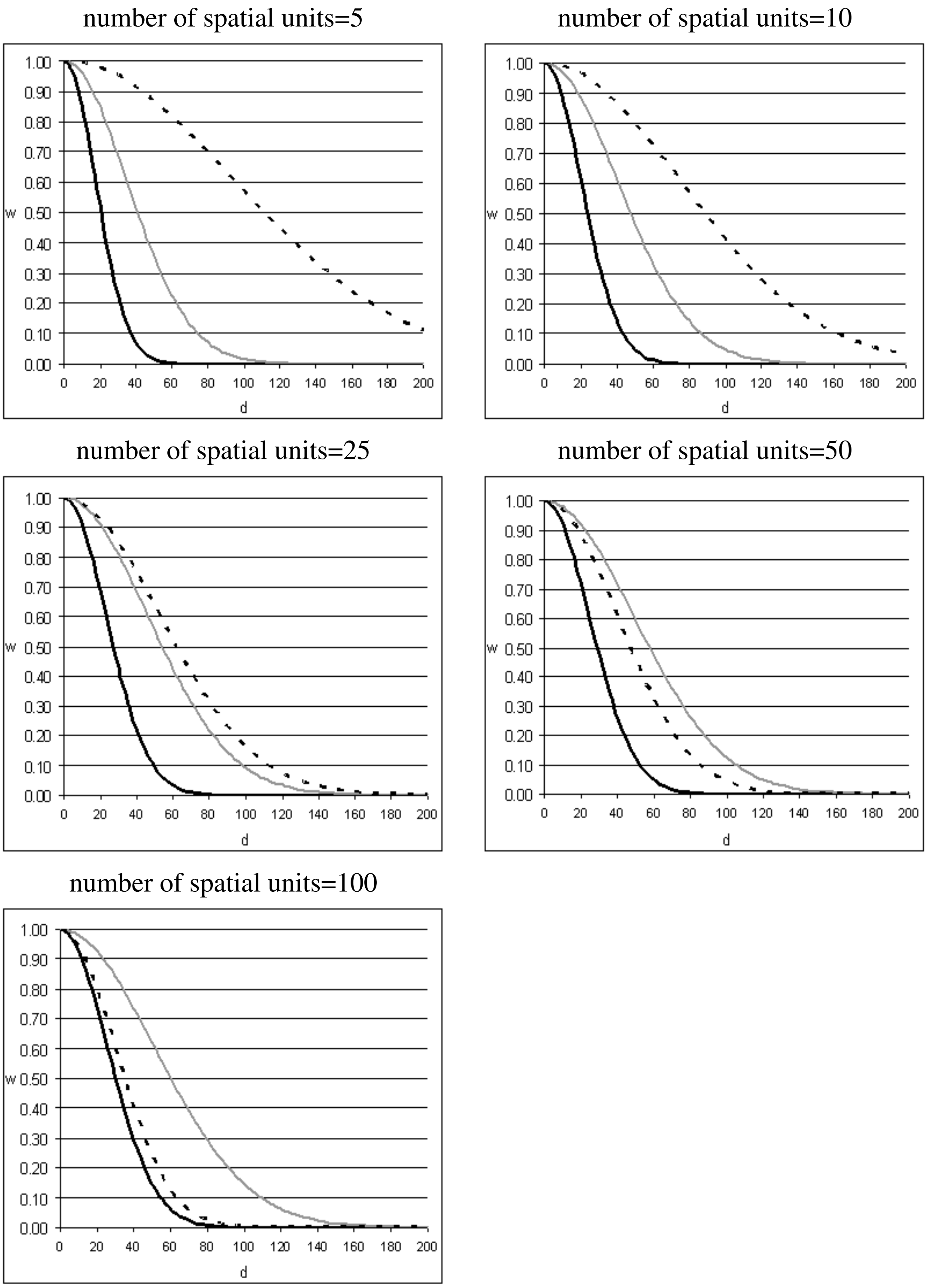

Figure 2: Repartition of Italy in (from darker to lighter): Northwest, Northeast, Central, Southern, Insular.

Figure 3: Regional Italian crude births: Conditional correlations of two pairs of Italian regions derived from the space–time model with h_{Mm} bandwidth.

A. Lombardy–Veneto

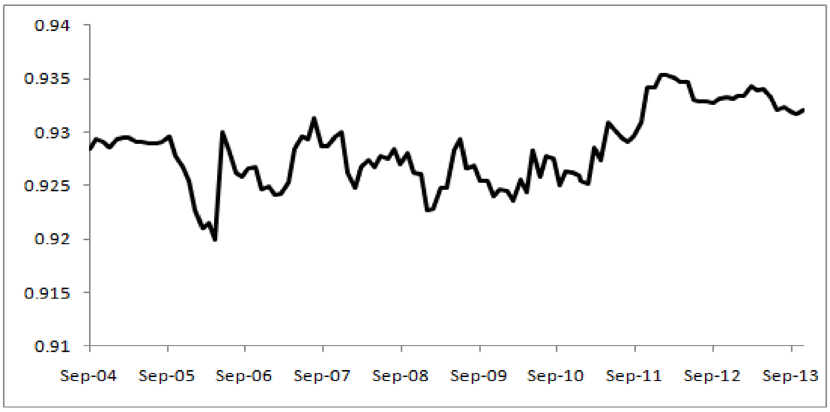

B. Valle d'Aosta–Lazio

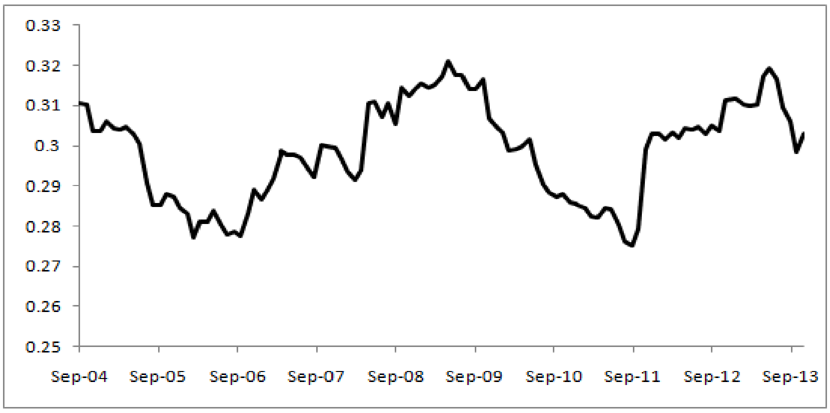

Figure 4: Dendrograms derived using the entries of Tables 5 (left panel) and 6 (right panel) as similarity measures.

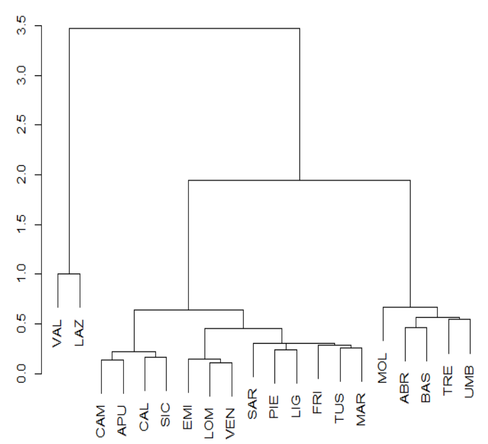

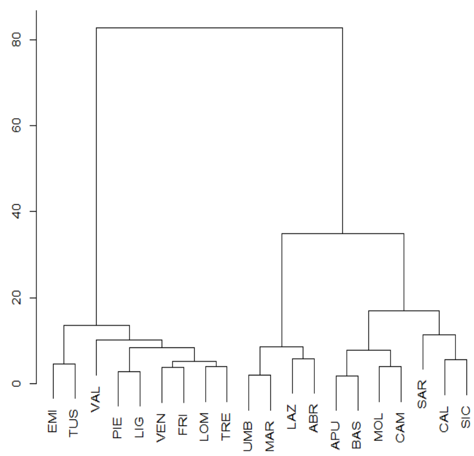

The dendrogram is generated using the Ward linkage method. The y–axis shows the distance at which the clusters combine. These distances are obtained by rescaling the calculated distances derived from Table 5 to 0 to 3.5 and from Table 6 to 0 to 80. The ratio of the rescaled distances within the dendrogram is the same as the ratio of the original distances.

Ultimi Contributi di Ricerca CRENoS

I Paper sono disponibili in: http://www.crenos.it

14/05 *Francesco Quatraro, Stefano Usai,* "Are knowledge flows all alike? Evidence from European regions"
14/04 *Angelo Antoci, Fabio Sabatini, Mauro Sodini* "Online and offline social participation and social poverty traps. Can social networks save human relations?"
14/03 *Anna Bussu, Claudio Detotto,* "The bi-directional relationship between gambling and addictive substances"
14/02 *Alessandro Fiori, Tadas Gudaitis,* "Optimal Individual Choice of Contribution to Second Pillar Pension System in Lithuania"
14/01 *Oliviero A. Carboni, Paolo Russu,* Measuring Environmental and Economic Efficiency in Italy: an Application of the Malmquist-DEA and Grey Forecasting Model
13/24 *Luca Deidda, José J. Cao-Alvira,* "Financial liberalization and the development of microcredit"
13/23 *Manuela Deidda,* "Economic hardship, housing cost burden and tenure status: evidence from EU-SILC"
13/22 *Vania Manuela Licio, Anna Maria Pinna,* "Measuring insularity as a state of nature. Is there a case of bad geography?"
13/21 *Vania Manuela Licio, Anna Maria Pinna,* "The European firms' export activity to the neighbouring countries"
13/20 *Kallioras Dimitris, Anna Maria Pinna,* "Trade activity between the EU and its neighboring countries: Trends and potential"
13/19 *Claudia Cigagna, Giovanni Sulis,* "On the potential interaction between labour market institutions and immigration policies"
13/18 *Romana Gargano, Edoardo Otranto,* "Financial Clustering in Presence of Dominant Markets"
13/17 *Ettore Panetti,* "Financial Liberalization with Hidden Trades"
13/16 *Adriana Di Liberto,* "Length of stay in the host country and educational achievement of immigrant students: the Italian case"
13/15 *Audrius Bitinas, Alessandro Fiori Maccioni* "Lithuanian pension system's reforms following demographic and social transitions"
13/14 *Guillermo Baquero, Malika Hamadi, Andréas Heinen* "Competition, Loan Rates and Information Dispersion in Microcredit Markets"
13/13 *Paul A. Bekker, Federico Crudu,* "Jackknife Instrumental Variable Estimation with Heteroskedasticity"
13/12 *Claudio Deiana,* "Health Shocks and Labour Transitions Across Europe"
13/11 *Stefano Usai, Emanuela Marrocu, Raffaele Paci,* "Networks, proximities and inter-firm knowledge exchanges"
13/10 *Claudio Detotto, Bryan C. McCannon, Marco Vannini*, "A Note on Marginal Deterrence: Evidence"
13/09 *Riccardo Marselli, Bryan C. McCannon, Marco Vannini*, "Bargaining in the Shadow of Arbitration"

Finito di stampare nel mese di Dicembre 2014
Presso Centro Stampa dell'Università degli Studi di Cagliari
Via Università 40
09125 Cagliari

www.crenos.it

ISBN 978-88-84-67-883-6